

介质 FC-770 受激布里渊散射脉冲压缩 Stokes 线宽特性研究 (特邀)

廉玉东^{1,2,3}, 胡 祺^{1,2}, 解璐洋^{1,2}, 靳 鹏^{1,2}, 杜奋娇^{1,2}, 王雨雷^{1,2}, 吕志伟^{1,2}

(1. 河北工业大学 先进激光技术研究中心, 天津 300401;

2. 河北省先进激光技术与装备重点实验室, 天津 300401;

3. 天津市电子材料与器件重点实验室, 天津 300401)

摘要: 布里渊散射是指入射到介质的泵浦光束与介质内的弹性声波声子发生相互作用而产生的三阶非线性光散射现象。在受激布里渊散射 (SBS) 脉冲压缩过程中, 时域脉宽压缩研究较为广泛, 但压缩过程中频域线宽变化与介质粘度、折射率等特性密切相关, 因此文中研究聚焦单池结构下 SBS 脉冲压缩过程中介质 FC-770 产生的 Stokes 线宽变化影响因素, 发现随着泵浦能量的增加, Stokes 线宽先迅速增加后逐渐压窄至 400 MHz 左右, 而随着产生池前透镜焦距的逐渐减小, Stokes 线宽迅速压窄, 且随能量变化线宽变化范围减小, 最后探究了入射激光线宽对 Stokes 线宽变化的影响因素, 得出介质 FC-770 产生的 Stokes 线宽值与入射激光线宽呈正比例关系, 入射激光线宽值由 280 MHz 变化到 450 MHz 左右时, 输出的 Stokes 线宽值由 500 MHz 变化到 680 MHz 左右。

关键词: 受激布里渊散射; 脉冲压缩; 线宽; 介质 FC-770

中图分类号: TN249 **文献标志码:** A **DOI:** 10.3788/IRLA20230402

0 引言

SBS 技术由于其能量转化效率高、布里渊频移较小和相位共轭等优点引起人们广泛的关注^[1-3]。目前, 受激布里渊散射技术已应用于布里渊光谱^[4-7]、脉宽压缩^[8]、光束整形^[9]等领域。其中布里渊频移和线宽是布里渊光谱中描述介质特性的两个重要参数, 布里渊频移和线宽已成功应用于区分介质种类、浓度和温度等特性信息^[10-12]。SBS 脉宽压缩技术大多关注于时域脉宽的变化情况^[13-14], 对频域线宽变化特性涉及较少^[15-16], 但频域线宽特性与介质粘度、温度、折射率密切相关, 因此探究 SBS 压缩过程中的线宽变化规律对于研究介质特性是必要的。

文中研究了 SBS 脉冲压缩过程中介质 FC-770 产生的 Stokes 线宽变化影响因素。由于 SBS 应用过程中激光重复频率较低, 因此实验选用法布里-珀罗 (Fabry-Pérot, F-P) 标准具结合光束质量分析仪 (COMS beam profilers, CBP) 法来准确测量低重复频率下的

Stokes 线宽变化, 最终探究了聚集单池结构下 SBS 脉冲压缩过程中线宽值变化, 并通过二级 SBS 压缩结构进行输入线宽控制, 整体分析了 SBS 脉冲压缩过程泵浦能量、透镜聚焦参数、输入线宽对 Stokes 线宽变化的影响规律, 对研究介质特性具有重要意义。

1 理论分析

在 SBS 过程中, Stokes 频率分量可由分布噪声起源模型^[17]推导得出:

$$s(\omega) = \frac{8\pi\hbar\omega_s(\bar{n}+1)}{ncA\Gamma} \left\{ \exp \left[\frac{G(\Gamma/2)^2}{\omega^2 + (\Gamma/2)^2} \right] - 1 \right\} \quad (1)$$

可得出增益系数 G 较高时, Stokes 线宽为^[17]:

$$\Delta\omega = \Gamma \left(\frac{\ln 2}{G - \ln 2} \right)^{1/2} \quad (2)$$

式中: Γ 为布里渊线宽; $G = gIl$, g 为介质布里渊增益系数, I 为泵浦光强度, l 为泵浦光与 Stokes 光相互作用长度。

当增益系数较小时, SBS 阈值附近 Stokes 线宽输

收稿日期: 2023-04-05; 修订日期: 2023-05-25

基金项目: 国家自然科学基金项目 (61905062, 61927815); 中国博士后科学基金项目 (2020M670613); 河北省博士后择优资助项目 (B2020003026)

作者简介: 廉玉东, 男, 副教授, 博士, 主要从事高功率全固态激光器及非线性光学方面的研究。

出为^[18]:

$$\Delta w = \left[\frac{G\Gamma^2}{\ln(e^G + 1)/2} - \Gamma^2 \right]^{1/2} \quad (3)$$

由公式可看出,在脉冲压缩过程中,Stokes 线宽与布里渊线宽 Γ 紧密相关^[19-20],布里渊线宽表达式为:

$$\Gamma = 1/(\pi \times \tau) \quad (4)$$

其中,介质声子寿命为:

$$\tau = \frac{\lambda^2}{16\pi^2 n^2 \eta} \quad (5)$$

式中: n 为介质折射率; η 为介质运动粘度。由此可以看出,当入射光波长一定时,声子寿命与介质的折射率和运动粘度成反比例关系。

2 实验及结果分析

2.1 实验装置

介质 FC-770 由于其具有较好的时域 SBS 压缩特性,因此探究其脉冲压缩过程中的 Stokes 线宽变化具有重要意义。实验装置如图 1 所示。图中,P 为偏振

片,HWP 为二分之一波片,R 为旋光器,QWP 为四分之一波片,L 为透镜,M 为反射镜,PBS 为偏振立方晶体,CBP 为光束质量分析仪。泵浦激光器为 1064 nm 脉冲激光器,脉冲宽度为 7.4 ns,重复频率在 1~10 Hz 范围内可调,输出能量由激光能量计探头 (OPHIRPE50 BB-DIF-C) 和表头 (OPHIR NOVA II) 测量。激光器单纵模率通过示波器时域输出波形和频域频率分布来确定,经过示波器 1000 次记录,单纵模率测量结果为 99% 左右。激光器输出线宽在 250 MHz 左右。由于 SBS 具有较强的返回光,因此偏振片 P_1 、 P_2 、半波片 HWP_2 和旋光器 R_1 共同组成空间光隔离装置以保护泵浦光源。 HWP_1 和 P_1 控制进入 SBS 产生池的泵浦能量,产生池设置为 1000 mm,产生池前放置聚焦透镜 L_1 。当泵浦光功率密度大于 SBS 产生阈值后,后向散射光光强快速增长,经半波片 HWP_3 、偏振立方晶体 PBS 和四分之一波片 QWP_2 共同控制进入 F-P 标准具的 Stokes 光能量,由 CBP 采集得到介质产生的 Stokes 干涉圆环。

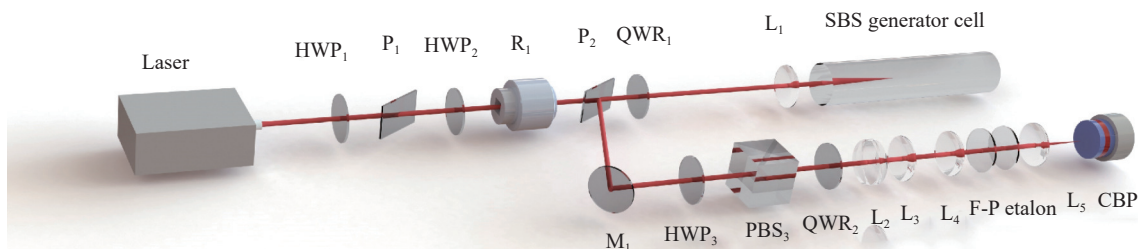


图 1 SBS 脉冲压缩实验装置

Fig.1 SBS pulse compression experimental setup

2.2 实验结果分析

当泵浦能量为 15 mJ, L_1 透镜焦距为 500 mm 时,由 CBP 采集得到介质 FC-770 产生的 Stokes 干涉圆环如图 2 所示。

通过霍夫变换精确识别干涉圆环圆心以提取过圆心的一组像元的灰度值来表征激光干涉谱线,图 3 为干涉圆环经过处理后得到的干涉散点图。

由于 F-P 标准具自身透射光谱的存在,干涉线宽值与激光本征线宽值之间存在一定误差,通过非线性拟合消除仪器误差可得到 Stokes 本征线宽值,线宽拟合结果为 553 MHz,结果如图 4 所示。

在 SBS 脉冲压缩过程中,泵浦能量、透镜焦距、

输入激光线宽都是 Stokes 线宽输出的重要影响因素。在输入线宽固定时,产生池前透镜焦距设置为 500 mm,通过改变泵浦能量对 SBS 压缩过程中 Stokes 光线宽变化进行了研究,实验结果如图 5 所示。可以看出,随着泵浦能量的增加,能量反射率呈现先快速增加,随着泵浦能量的进一步增大,泵浦光与 Stokes 光耦合作用的增强并不明显,在能量反射率达到 60% 后,能量反射率增长逐渐缓慢。在泵浦能量增大的过程中,可以看到 Stokes 线宽先迅速增大,后逐渐减小,这是由于泵浦能量开始增大时增益系数较小,焦点功率密度迅速上升,导致线宽急剧展宽,此时泵浦能量为 10 mJ 时,Stokes 线宽值达到 580 MHz 左

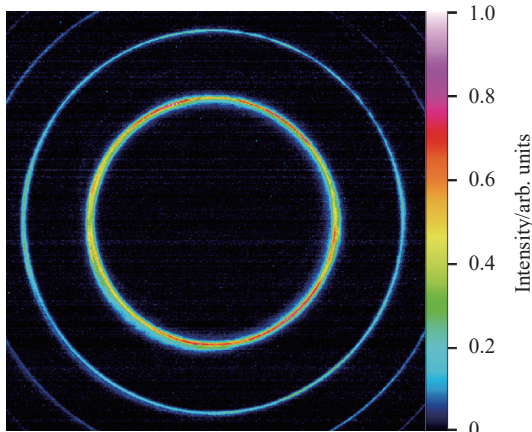


图 2 CBP 采集的干涉圆环图

Fig.2 Interference circles captured using CBP

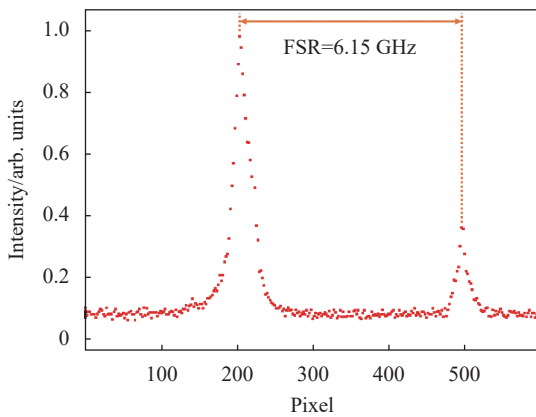


图 3 光谱散点图

Fig.3 Spectral scatter plot

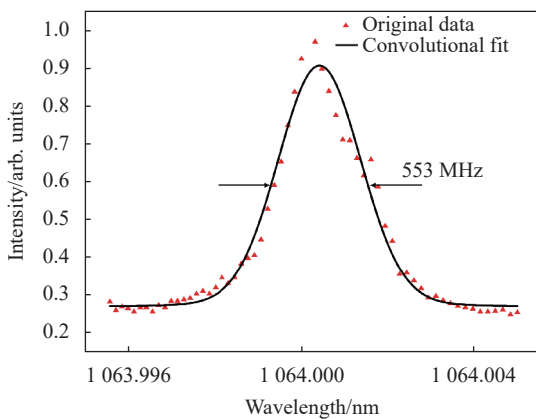


图 4 非线性拟合结果

Fig.4 Non-linear fit results

右。当泵浦能量进一步增加时,增益系数逐渐增大,随着焦点处能量密度的增加,Stokes 线宽逐渐压窄,当泵浦能量为 35 mJ 时,Stokes 线宽可压窄至 400 MHz

左右,随着泵浦能量的增大,Stokes 线宽压窄效果趋势减小,这可以解释为 Stokes 脉冲随着泵浦能量的增加提取效率逐渐趋于饱和,线宽变化趋势减缓。

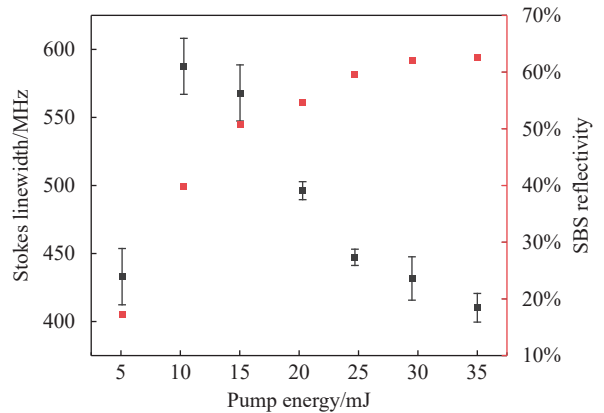


图 5 Stokes 线宽和能量反射率随泵浦能量的变化

Fig.5 Variation of Stokes linewidth and energy reflectivity with pumping energy

在 SBS 压缩过程中,除了泵浦光能量直接影响焦点处的功率密度,透镜聚焦参数也是重要影响因素。图 6 显示了不同焦距、不同能量下介质 FC-770 产生的 Stokes 线宽变化情况。由实验结果可以得出随着透镜焦距的减小,Stokes 输出线宽变窄,且随着能量的增加,可以看到 Stokes 线宽压窄效果并不明显。当泵浦能量为 30 mJ,透镜焦距为 150 mm 时,Stokes 线宽可压窄至 300 MHz 左右,当焦距为 300 mm 时 Stokes 线宽值为 325 MHz 左右,透镜焦距为 500 mm 时 Stokes 线宽值为 430 MHz 左右,这是由于随着透镜焦距的增加,焦点处的能量密度减小,但透镜焦距的增加使泵浦光与反向传输的 Stokes 光有效相互作用长度增加,

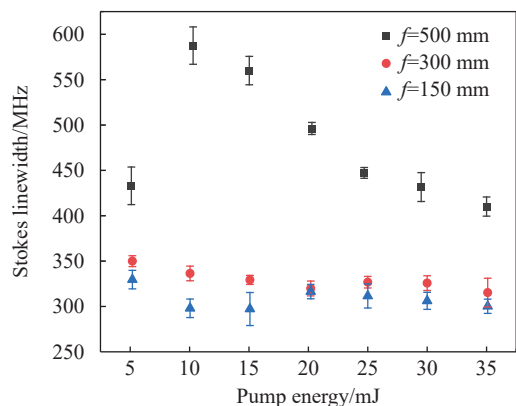


图 6 Stokes 线宽随透镜焦距的变化

Fig.6 Variation of Stokes linewidth with the focal length of the lens

Stokes 脉冲可有效提取泵浦光能量,使得相互作用过程中,增益系数较大,Stokes 线宽迅速增加。

当泵浦能量和透镜焦距一定时,该实验采取紧凑双池脉冲压缩结构来控制入射到产生池的激光线宽,实验装置如图 7 所示。实验采取紧凑双池控制线宽

变化是因为紧凑双池结构在 SBS 压缩过程中输出时域脉冲波形尾部调制现象并不明显,排除时域脉冲波形样貌对线宽造成影响,且紧凑双池结构能量转换效率更高。设置此时入射到第二级产生池的能量为 13 mJ 左右,产生池透镜 L_2 焦距设置为 500 mm。

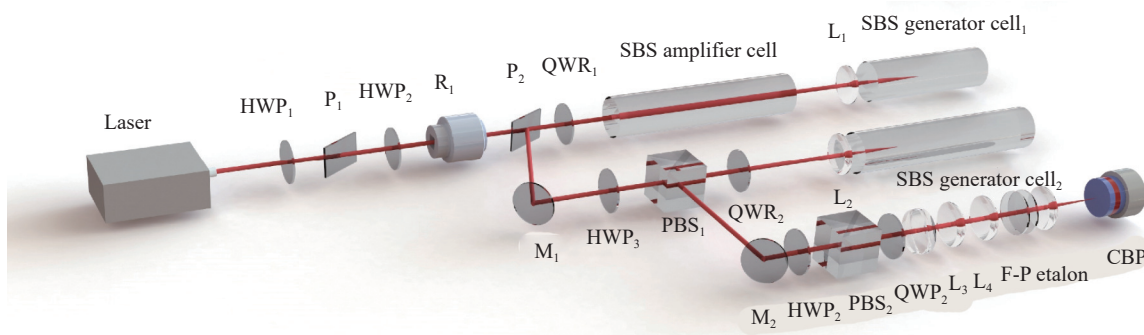


图 7 两级 SBS 脉冲压缩实验装置

Fig.7 Two-stage SBS pulse compression experimental setup

通过改变入射到第二级产生池的线宽值,对 SBS 压缩过程中介质 FC-770 产生的 Stokes 光线宽变化进行了研究,实验结果如图 8 所示。由实验结果可以看出,入射到第二级产生池的线宽值由 280 MHz 变化到 450 MHz 左右时,输出的 Stokes 线宽值由 500 MHz 变化到 680 MHz 左右。随着入射到第二级产生池的线宽值逐渐增加,输出的 Stokes 线宽值逐渐增加,整体呈正相关趋势,但入射线宽值较大时,Stokes 线宽值增大趋势减缓。

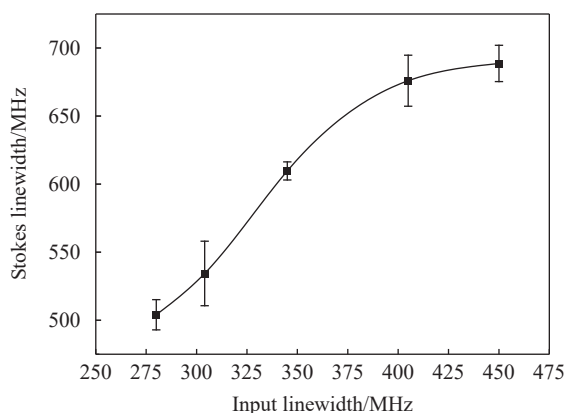


图 8 Stokes 线宽随入射线宽值的变化

Fig.8 Variation of Stokes linewidth with the value of incident linewidth

3 结论

综上所述,文中探究了介质 FC-770 在 SBS 脉冲

压缩过程中 Stokes 线宽变化的影响因素,发现 Stokes 输出线宽变化随着泵浦功率密度的增加呈现先增加后迅速压窄的趋势。随着产生池前透镜焦距的减小,Stokes 线宽变窄,且当透镜焦距较小时,Stokes 线宽变化受泵浦能量影响效果减弱。通过二级压缩控制输入激光线宽,随着入射线宽值的增加,Stokes 输出线宽逐渐展宽。由于以往的 SBS 压缩工作对频域线宽的变化涉及较少,但 SBS 压缩过程中线宽值变化具有特定规律,且频域线宽变化包含了丰富的介质特性信息,因此研究 SBS 压缩过程中 Stokes 线宽变化对于介质特性研究具有重要意义。

参考文献:

- [1] Bai Z, Yuan H, Liu Z, et al. Stimulated Brillouin scattering materials, experimental design and applications: A review [J]. *Optical Materials*, 2018, 75: 626-645.
- [2] Wang Yulei. Investigation on a 100-J laser system and high-energy and high-power stimulated Brillouin scattering phase conjugation[D]. Harbin: Harbin Institute of Technology, 2007. (in Chinese)
- [3] Wang Tianqi, Kang Zhijun, Meng Dongdong, et al. Application progress of the stimulated Brillouin scattering phase conjugate mirror in high power nanosecond lasers [J]. *Infrared and Laser Engineering*, 2021, 50(5): 20211024. (in Chinese)
- [4] Remer I, Shaashoua R, Shemesh N, et al. High-sensitivity and high-specificity biomechanical imaging by stimulated Brillouin

- scattering microscopy [J]. *Nature Methods*, 2020, 17(9): 913-916.
- [5] Krug B, Koukourakis N, Guck J, et al. Nonlinear microscopy using impulsive stimulated Brillouin scattering for high-speed elastography [J]. *Optics Express*, 2022, 30(4): 4748-4758.
- [6] Xu Jiaqi, Wang Yuanqing, Xu Yangrui, et al. Research progress of ocean environmental laser remote sensing based on Brillouin scattering [J]. *Infrared and Laser Engineering*, 2021, 50(6): 20211036. (in Chinese)
- [7] Zhang Yi, Bai Lianfa, Chen Qian, et al. Application of Brillouin scattering on underwater laser imaging detection [J]. *Infrared and Laser Engineering*, 2009, 38(4): 665-668, 678. (in Chinese)
- [8] Lian Yudong, Wang Yuhe, Zhang Yuqin, et al. Research progress of stimulated Brillouin scattering pulse compression technique [J]. *High Power Laser and Particle Beams*, 2021, 33(5): 051001. (in Chinese)
- [9] Scott A M, Ridley K D. A review of Brillouin-enhanced four-wave mixing [J]. *IEEE Journal of Quantum Electronics*, 1989, 25(3): 438-459.
- [10] O'Connor S P, Doktor D A, Scully M O, et al. Impulsive stimulated Brillouin spectroscopy for assessing viscoelastic properties of biologically relevant aqueous solutions[C]//SPIE, 2021, 11645: 11645A.
- [11] Hua Dengxin, Wang Jun. Research progress of ocean laser remote sensing technology(invited) [J]. *Infrared and Laser Engineering*, 2018, 47(9): 0903003. (in Chinese)
- [12] Xu Meng, Niu Haisha, Zhu Lianqing, et al. Elastic modulus measurement based on virtual image phase array confocal Brillouin spectroscopy technology [J]. *Infrared and Laser Engineering*, 2021, 50(4): 20200265. (in Chinese)
- [13] Liu Z, Fan R, Jin D, et al. Quarter acoustic period pulse compression using stimulated Brillouin scattering in PF-5060 [J]. *Optics Express*, 2022, 30(8): 12586-12595.
- [14] Liu Z H, Wang Y L, Wang Y R, et al. Pulse-shape dependence of stimulated Brillouin scattering pulse compression to sub-photon lifetime [J]. *Optics Express*, 2018, 26(5): 5701-5710.
- [15] Wang J, Bai Z, Hun X, et al. Stokes linewidth narrowing by stimulated Brillouin scattering in liquid media [J]. *Applied Physics Express*, 2023, 16(1): 012014.
- [16] Zhang Dong, Zhang Lei, Shi Jiulin, et al. Line width compression and temporal coherence of stimulated Brillouin scattering [J]. *Acta Physical Sinica*, 2012, 61(6): 064212. (in Chinese)
- [17] Boyd R W, Rzaewski K, Narum P. Noise initiation of stimulated Brillouin scattering [J]. *Physical Review A*, 1990, 42(9): 5514.
- [18] Yeniay A, Delavaux J M, Toulouse J. Spontaneous and stimulated Brillouin scattering gain spectra in optical fibers [J]. *Journal of Lightwave Technology*, 2002, 20(8): 1425-1432.
- [19] Prevedel R, Diz-muñoz A, Ruocco G, et al. Brillouin microscopy: an emerging tool for mechanobiology [J]. *Nature Methods*, 2019, 16(10): 969-977.
- [20] Wang Xueyang. Research on the compression properties for generating SBS pulse of hundreds picosecond[D]. Harbin: Harbin Institute of Technology, 2013. (in Chinese)

Research on the Stokes linewidth characteristics of the pulse compression by stimulated Brillouin scattering in medium FC-770 (invited)

Lian Yudong^{1,2,3}, Hu Qi^{1,2}, Xie Luyang^{1,2}, Jin Peng^{1,2}, Du Fenjiao^{1,2}, Wang Yulei^{1,2}, Lv Zhiwei^{1,2}

(1. Center for Advanced Laser Technology, Hebei University of Technology, Tianjin 300401, China;

2. Hebei Key Laboratory of Advanced Laser Technology and Equipment, Tianjin 300401, China;

3. Tianjin Key Laboratory of Electronic Materials and Devices, Tianjin 300401, China)

Abstract:

Objective Brillouin scattering is a third-order nonlinear light scattering phenomenon resulting from the interaction of a pump beam incident on a medium with elastic acoustic phonons within the medium. The stimulated Brillouin scattering (SBS) technique is widely used for its high-energy conversion efficiency, small Brillouin frequency shift, and phase conjugation. Currently, the SBS technique has been widely used in Brillouin spectroscopy, pulse width compression, and beam combination, in which the frequency shift and linewidth are two essential parameters of Brillouin scattering. The frequency shift and linewidth have been successfully applied in Brillouin spectroscopy to differentiate the information about medium type, concentration, and temperature

characteristics. Previous studies mainly focus on measuring time-domain pulse width in SBS pulse-width compression. The study of frequency-domain linewidth variation is less involved. In contrast, the linewidth variation characteristics are closely related to the information about medium viscosity, temperature, and refractive index, so it is of great significance to investigate the linewidth variation characteristics during SBS compression.

Methods The experiment probes the linewidth change of the medium FC-770 during SBS compression by focusing a single-cell setup, which is mainly composed of a generator and a long focusing lens and is characterized by controllable incident energy and a simple structure. The linewidth change incident to the second-stage generator is controlled by the compact two-cell setup, which has high-energy conversion efficiency, and the time-domain waveform of the incident pulse generated by the compact two-cell setup can maintain a better shape to avoid the effect of the time-domain waveform on the linewidth change. Due to the low laser repetition frequency during SBS compression, the Fabry-Pérot (F-P) combined with the COMS beam profilers (CBP) is selected to measure Stokes linewidth at low repetition frequency. The interference scattering plot is obtained by processing the interference circle acquired by CBP, and the Stokes intrinsic linewidth value is obtained after non-linear fitting.

Results and Discussion During the SBS compression, pump energy, lens focusing parameters, and incident laser linewidth influence the Stokes linewidth output. With the increase of the pump energy, the energy reflectivity increases rapidly, and the Stokes linewidth first increases rapidly and then gradually narrows. When the pump energy is 35 mJ, the Stokes linewidth can be narrowed to about 400 MHz (Fig.5). As the focal length of the lens increases, the energy density at the focal point decreases, but the increase in focal length of the lens increases the effective interaction length of the pump light with the back-transported Stokes light, and the Stokes linewidth increases rapidly (Fig.6). By taking a compact two-cell setup to control the linewidth incident to the generator, it can be seen that as the value of the linewidth incident to the second-stage generator gradually increases, the value of the output Stokes linewidth gradually increases, and when the value of the linewidth incident to the second-stage generator varies from 280 MHz to about 450 MHz, the value of the output Stokes linewidth varies from 500 MHz to about 680 MHz (Fig.8).

Conclusions During the SBS compression process, the variation of the Stokes linewidth of the medium FC-770 output shows a tendency of first increasing and then rapidly narrowing with the increase of the pump power density. As the lens's focal length in front of the generator decreases, the Stokes linewidth becomes narrower. When the focal length of the lens is small, the Stokes linewidth variation is less effective by the pump energy. The input laser linewidth is controlled by secondary compression, and the Stokes output linewidth gradually broadens as the incident linewidth value increases. From the experiments, it can be seen that the linewidth variation in the SBS compression process has a specific law, and the frequency domain linewidth variation contains rich information about the medium properties, so the study of Stokes linewidth variation in the SBS compression process is of great significance for the study of medium properties.

Key words: stimulated Brillouin scattering; pulse compression; linewidth; medium FC-770

Funding projects: National Natural Science Foundation of China (61905062, 61927815); China Postdoctoral Science Foundation (2020M670613); Hebei Postdoctoral Scholarship Project (B2020003026)